GLOBAL OPTIMIZATION AND ANTENNAS SYNTHESIS AND DIAGNOSIS, PART TWO: APPLICATIONS TO ADVANCED REFLECTOR ANTENNAS SYNTHESIS AND DIAGNOSIS TECHNIQUES

A. Capozzoli and G. D'Elia

Dipartimento di Ingegneria Elettronica e delle Telecomunicazioni
Università di Napoli "Federico II"
Via Claudio, 21, 80125 Napoli, Italia

Abstract—The paper presents the application of the hybrid global optimization algorithm, introduced in the companion paper Part I, to reflector antenna power pattern synthesis and reflector antenna surface diagnosis from only amplitude data. The synthesis algorithm determines both the reflector surface and the excitation coefficients of the array of primary feeds to meet the designing specification on the far-field pattern expressed by means of two couple of masks bounding the squared amplitude of both the copolar and crosspolar components. The diagnosis technique allows to find the reflector surface profile from the measurement of the far field power pattern by a proper formulation of the corresponding inverse problem. In both cases we take advantage of the exploring capability of an evolutionary algorithm and of the solution refinement capability of an efficient, quasi-Newton based, local search procedure. The numerical analysis shows that Global Optimization can outperform the standard local approach, by significantly improving the performance of the synthesized antenna in the first case and by enhancing the reliability of the diagnosis procedure in the second one.

1. INTRODUCTION

The solution of the power pattern antenna synthesis problem and of the antenna diagnosis from only amplitude field data requires the global optimization of a non linear multimodal objective functional.

In many instances, such optimization problems are afforded by exploiting a local optimization technique.

However, as explained in the Part I of this paper, this approach suffers from the trapping problem due to the secondary minima of the objective functional leading the searching algorithm into false solutions.

Accordingly, new strategies able to overcome or significantly reduce the occurrence of false solutions have been introduced in Part I and are here exploited.

In particular, the aim of the paper is to present the applications of a global optimization algorithm to reflector antennas power pattern synthesis and reflector antennas surface diagnosis from amplitude only far field data. These are two problems of real interest in the electromagnetic community as long as high performances are required in modern telecommunication and radar applications.

As long as antenna synthesis is considered, it must be noted that sophisticated synthesis procedures are mandatory to effectively exploit, at the designing stage, all the degrees of freedom in the radiating structure and to meet at best the user's needs. In recent years the problem has been stated in a general and flexible mathematical framework leading to an effective synthesis technique for scanning and/or reconfigurable hybrid antennas also with near-field constraints [1–18].

However, the use of local optimization procedures, can miss the best attainable solution wasting the potentiality of the radiating system and of the synthesis approach [19–26].

Once the antenna has been designed and carried out, reliable and accurate diagnosis procedures are required to monitor the system and collect those information needed to restore the optimum working conditions. As a matter of fact, the performances of reflector antennas are strongly degraded by the distortions of the primary reflecting surface, misalignments of the antenna feed as well as of the subreflector [27, 28].

Accordingly, antenna diagnosis techniques, possibly simple and inexpensive, are required. Convenient approaches retrieve the state parameters of the radiating system useful in the restoring process by measuring the field radiated by the antenna [28–50]. To avoid the difficulties related to the phase measurement, diagnosis techniques exploiting only amplitude field data have been developed [50, 36, 38, 39, 42, 44, 45, 49]. Again, since these approaches are based on the optimization of a multiextremal functional, global optimizers are required in order to attain a reliable estimation of the antenna status [51–54, 43].

In this paper we firstly present the mathematical framework of the antenna synthesis and diagnosis problem, then the optimization

algorithm is applied and the results of the numerical analysis are discussed by comparing the obtained results with those achievable by using a local optimization approach.

2. PROBLEM FORMULATION

In the Part I of the paper, we showed that the optimization of multiextremal functions by means of standard techniques of local nature can lead to a totally useless estimation of the searched solution.

We also noted that the rapid evolution of Global Optimization, both from a theoretical and an algorithmic point of view, together with the impressive growing of the computational resources nowadays available, provided effective tools to look for global optima.

Moreover, we also stressed that the effective performances of Global Optimization techniques in practical applications can be evaluated only if these algorithms are tested against real world problems.

In this Part II of the paper, we present two different applications of a Hybrid Evolutionary Algorithm to relevant topics in applied electromagnetics.

The first example considers the synthesis of hybrid reflector antennas, i.e., the synthesis of contoured-beam reflector antennas fed by an array of primary sources.

The second example concerns the diagnosis of large reflector antennas from far-field, only amplitude, data.

In both cases the numerical analysis shows that Global Optimization can outperform the standard local approach, by significantly improving the performance of the synthesized antenna in the first case and by enhancing the reliability of the diagnosis procedure in the second one.

For the sake of convenience, to address the two problems, a common mathematical framework, naturally leading to an optimization problem, will be exploited [1].

In fact, in both cases, we need to find a set of parameters defining the working state of the radiating system:

  a) the design parameters, in the synthesis case, to be determined to meet the design specifications;

  b) the diagnosis parameters, in the diagnosis case, to be determined to match the measured data.

Accordingly, we can define two functional spaces, $\mathcal{X}$ and $\mathcal{Y}$ say. The space $\mathcal{X}$ represents the set wherein the unknown state parameters, say $\underline{X}$, defining the properties of the radiating system lie. The space $\mathcal{Y}$

represents the set to which the system output, say $\underline{Y}$, belongs, i.e., the radiated pattern or the observed data in the synthesis or diagnosis case, respectively.

Moreover, it is convenient to model the antenna system by introducing the operator A

$$\mathsf{A} \mid \underline{X} \in \mathsf{X} \to \underline{Y} \in \mathsf{Y} \tag{1}$$

However, in any practical problem, physical constraints as well as design specifications usually require that $\underline{X}$ belongs to a subset, say $\mathcal{X}_c$, of $\mathcal{X}$.

Analogously, design specifications, in the synthesis case, or measurement errors and noise, in the diagnosis case, require that $\underline{Y}$ belongs to a subset, say $\mathcal{Y}_c$, of $\mathcal{Y}$, rarely reducing to a singleton. And so, in both cases the goal of the procedure is to find a point in the intersection set:

$$\mathsf{A}(\mathsf{X_c}) \cap \mathsf{Y}_c \tag{2}$$

where $\mathsf{A}(\mathsf{X_c})$ is the image of $\mathcal{X}_c$ through the operator A.

Provided that $\mathcal{Y}_c$ is a closed set, this is equivalent to find a point $\hat{\underline{X}} \in \mathcal{X}_c$ such that:

$$d^2(\mathsf{A}(\hat{\underline{X}}), \mathsf{Y}_c) = \inf_{\underline{Y} \, \in \, \mathsf{Y}_c} \|\mathsf{A}(\hat{\underline{X}}) - \underline{Y}\|^2 = 0 \tag{3}$$

where $\| \cdot \|$ is a properly chosen norm equipping the space $\mathcal{Y}$ and $d^2(\underline{T}, \mathsf{Y}_c) = \inf_{\underline{Y} \, \in \, \mathsf{Y}_c} \|\underline{T} - \underline{Y}\|^2_{\mathsf{L}_2(\Omega)}$ denotes the squared distance of the element $\underline{T} \in \mathcal{Y}_c$ from $\mathcal{Y}_c$.

Accordingly, denoting with $\mathsf{P}_{\mathsf{Y}_c}$ the projector onto the set $\mathcal{Y}_c$, i.e., the operator that maps each element of $\mathcal{Y}$ onto the nearest element of $\mathcal{Y}_c$, $\hat{\underline{X}}$ can be obtained by solving the problem $\arg \min_{\mathsf{X_c}} F(\underline{X})$ with

$$F(\underline{X}) = \|\mathsf{A}(\underline{X}) - \mathsf{P}_{\mathsf{Y}_c}\mathsf{A}(\underline{X})\|^2 \tag{4}$$

It must be noted that, $\mathsf{A}(\mathsf{X_c}) \cap \mathsf{Y}_c$ can be a void set. F.i., this can be due to the approximations generally made when modeling the antenna system or, in the synthesis problem, to too tight design requirements. In this case, the global minimization of the functional (4) provides a quasi-solution to the inverse problem for the operator A [55].

This general framework will be now particularized to the synthesis and diagnosis problems.

2.1. Synthesis of Reflector Antennas

For the sake of simplicity, in the following we will consider a symmetrically fed reflector antenna with a fixed circular aperture, say
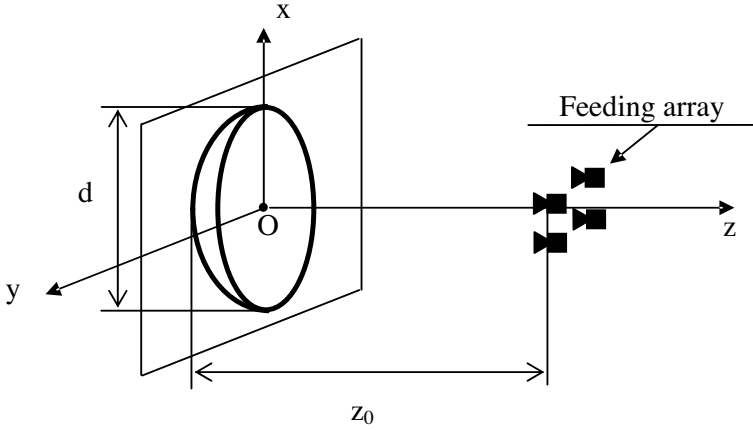
Figure 1. Geometry of the problem.

Σ, with diameter d, even if the extension of the approach to off-set antennas is straightforward.

By referring to the geometry depicted in Fig. 1, let us introduce a reference system (O, x, y, z) with the origin in the aperture plane $z = 0$ and consider a reflecting surface represented by a continuous function $z = Z(x, y)$ and a primary feed made by a planar array of a given number of elements aligned on a regular x-y grid and located on the plane $z = z_0$.

Assuming and dropping a time dependence $\exp(j\omega t)$, the far-field pattern, say $\underline{E}$, can be expressed as:

$$\underline{E}(u, v) = -jr\frac{\exp(j\beta r)}{\lambda}\underline{E}'(u, v) \qquad (5)$$

where $\underline{E}'(u, v)$ is the radiated far-field, (r, θ, φ) are the spherical coordinates, $u = \sin(\theta)\cos(\varphi)$, $v = \sin(\theta)\sin(\varphi)$, λ the wavelength and $\beta = \frac{2\pi}{\lambda}$.

The goal of the synthesis procedure is to evaluate the reflector shape, i.e., $Z(x, y)$, and the vector $\underline{c}$ of the excitation coefficients of the array elements that provide a far-field pattern meeting the design specifications. In the following, these specifications, involving a given portion, say Ω, of the (u, v) plane, will be expressed by means of two masks bounding the squared amplitude of the far-field co-polar and cross-polar components. Such components are denoted with E_{co} and E_{cr}, respectively. Each mask is defined by the upper and lower bound functions denoted by M_{co}^u and M_{co}^l, respectively, for the copolar component and M_{cr}^u and M_{cr}^l, for the crosspolar one.

Let us consider now the functional spaces $\mathcal{X}$ and $\mathcal{Y}$, the set $\mathcal{Y}_c$ and the operators A and $\mathsf{P}_{\mathsf{Y}_c}$ involved in Eq. (4).

Since the output of the antenna systems is given by the couple of the squared amplitudes of the co-polar and cross-polar components of the far-field, we set:

$$\mathsf{Y} = \{(T_1, T_2) \in \mathcal{L}_2(\Omega) \times \mathcal{L}_2(\Omega) \mid T_1(u,v) \geq 0, \, T_2(u,v) \geq 0 \, (u,v) \in \Omega\}$$
$$(6)$$

where $\mathcal{L}_2(\Omega)$ is the Hilbert space of square integrable functions over Ω and

$$\mathsf{Y}_c = \left\{ \begin{array}{l} (T_{co}, T_{cr}) \in \mathsf{Y} \mid \\ M_{co}^l(u,v) \leq T_{co}(u,v) \leq M_{co}^u(u,v) \, (u,v) \in \Omega \\ M_{cr}^l(u,v) \leq T_{cr}(u,v) \leq M_{cr}^u(u,v) \, (u,v) \in \Omega \\ T_{co}(u,v) = 0, \, T_{cr}(u,v) = 0 \quad \text{elsewhere} \end{array} \right\} \qquad (7)$$

It must be noted that the values of the elements of $\mathcal{Y}_c$ outside Ω have been set equal to zero in order to get beneficial effects on the well-position of the problem.

Concerning the definition of the operator A, it is noted that, since Global Optimization is a computational expensive task, particularly when several tens of real variables are involved, the demand for analytical tools avoiding time consuming approaches must be taken into account.

The synthesis method outlined in [2] and based on the aperture-approach seems to fit our needs and will be briefly recalled later on.

First, a convenient factorization of the aperture field $\underline{E}_a$ is considered, namely:

$$\underline{E}_a(\xi,\eta) = P_\Sigma(\xi,\eta) \exp\left(-j2\pi\left(\hat{L}(\xi,\eta) + S(\xi,\eta)\right)\right) \sum_l^n {}_k c_k \underline{V}_k(\xi,\eta)$$
$$(8)$$

where P_Σ is the support function of the reflector aperture Σ, L is the optical path, normalized to λ, from the center of the feeding array to the reflector aperture along the congruence of the incident and reflected rays, $\hat{L}$ is a normalized reference path, $S(\xi,\eta) = L(\xi,\eta) - \hat{L}(\xi,\eta)$, and $\underline{V}_k$ is the residual contribution to $\underline{E}_a$ due to the unitary excited k-th element of the feed array.

Then, to allow an effective numerical implementation and reduce the number of unknowns, a modal representation of S is adopted:

$$S = \underline{s} \cdot \underline{U} = \sum_l^p {}_i s_i U_i \qquad (9)$$

where $\{U_i\}_{i\in\mathsf{N}}$ is a complete sequence in $\mathcal{L}_2(\Sigma)$, N is the set of natural numbers and p is the number of the expansion terms.

As a consequence, the antenna input-output relationship involves the couples $(\underline{c}, \underline{s})$ and $(|E_{co}|^2, |E_{cr}|^2)$ and can be expressed by means of the operator A such that:

$$\mathsf{A}\,\mathsf{I}(\underline{s}, \underline{c}, \underline{V}) \rightarrow \left(|E_{co}|^2, |E_{cr}|^2\right) \tag{10}$$

where $\underline{V} = (\underline{V}_1, \ldots, \underline{V}_p)$.

The operator A can be conveniently evaluated by exploiting the computationally inexpensive Fourier transform relationship.

However, it must be stressed that eq. (10) uses an improper notation. In fact, S and $\underline{V}$, hence $\underline{s}$ and $\underline{V}$, are not independent on each other, since both depend on the reflector geometry and, thus, cannot be arbitrarily assigned. However, the dependence of $\underline{V}$ on the reflector shape Z is weaker than the dependence of S. And so, the design process suggested in [2] is performed by the following iterative scheme:

a) a reference reflector is chosen and the corresponding value of $\hat{L}$ is computed;

b) the value of $\underline{V}$ corresponding to the reference reflector, say $\hat{\underline{V}}$, is evaluated;

c) a couple $(\underline{c}, \underline{s})$ is determined by inverting the operator A in eq. (10), assuming $\underline{V}$ fixed and equal to $\hat{\underline{V}}$;

d) the reflector shape Z is obtained by inverse GO from the value of $\underline{s}$ obtained at point c).

It is noted that, to account for a possible relevant difference between $\underline{V}$ and $\hat{\underline{V}}$ during the iterations needed to perform step c), the reference reflector, and thus $\hat{\underline{V}}$, can be periodically updated. In this case the updated values of $\hat{L}$ and $\hat{\underline{V}}$ are the one corresponding to the reflector shape synthesized at the previous iteration.

It must noted that, to apply the GO laws at point d), the optical path L must satisfy the eikonal equation. Accordingly, in principle, we must face a constrained minimization of F by requiring that $S \in \mathsf{S}$ with

$$\mathsf{S} = \left\{ S \in C^l(\Sigma) | \nabla_{\xi\eta}(\hat{L} + S)I \leq 1 \right\} \tag{11}$$

$\nabla_{\xi\eta}$ denoting the transverse gradient operator in the normalized variables (ξ, η).

A further constraint is considered in [2] to account for spillover losses.

Following [2], to face the constrained minimization, the penalty method is applied. Accordingly, the inverse problem for the operator A at point c) can be solved by exploiting the general approach described at the beginning of the Section, by setting $\underline{X} = (\underline{c}, \underline{s})$, $\mathsf{X} = \mathsf{C}^{n_0} \times \mathsf{C}^p$ and minimizing the functional[†]:

$$F_{\alpha_1, \alpha_2}(\underline{s}, \underline{c}) = \|\mathsf{A}(\underline{s}, \underline{c}) - \mathsf{P}_{\mathsf{Y}_c}\mathsf{A}(\underline{s}, \underline{c})\|^2_{\mathsf{L}_2(\Omega, W) \times \mathsf{L}_2(\Omega, W)} + \alpha_1 Q_1(\underline{s}) + \alpha_2 Q_2(\underline{c})$$
(12)

where

$$Q_1(\underline{s}) = \left\| P_\Sigma \left| \nabla_{\xi\eta}\left(\hat{L} + \underline{s}\cdot\underline{U}\right)\right|^2 - P_\Sigma P_\infty \left|\nabla_t\left(\hat{L} + \underline{s}\cdot\underline{U}\right)\right|^2 \right\|^2_{\mathsf{L}_2(\Sigma)}$$
(13a)

$$Q_2(\underline{c}) = \left\| \left|\underline{E}_f\right|^2 \right\|^2_{\mathsf{L}_s(\Phi)}$$
(13b)

P_∞ is the operator projecting $|\nabla_{\xi\eta}S|^2 = |\nabla_{\xi\eta}(\underline{s}\cdot\underline{U})|^2$ (as an element of the space of square integrable functions) onto the sphere of unitary radius in the uniform norm, $\underline{E}_f$ is the field radiated by the primary feed array and Φ is the angular sector centered on the feed and not subtended by the reflector and α_1 and α_1 are two factors chosen to make the contributions of $Q_1(\underline{s})$ and $Q_2(\underline{c})$ comparable to the first term in eq. (12).

It is noted that the constant argument $\hat{\underline{V}}$ within A has been dropped out in eq. (12).

2.2. Diagnosis of Reflector Antennas

As mentioned above, the second application of a Hybrid Evolutionary Algorithm to Global Optimization here considered involves the diagnosis of reflector antennas from amplitude only far field data.

The aim of such a technique is to determine the working status of large reflector antennas for space and astronomical applications without requiring the complex set-up needed by the holographic techniques. In particular, both the misalignment of the primary feed and/or of the subreflector as well as the misalignment of the panels making up the primary reflecting surface must be retrieved. As shown in [46], the information for the antenna reset can be obtained once the phase of the field on the reflector aperture is assigned. In fact, the misalignment of the primary feed and of the subreflector can be evaluated by fitting the aperture phase with the best paraboloid. On

---

[†] We denote with $\mathcal{L}_2(\Omega, W)$ the space of square integrable functions over Ω with respect to a weighting function W. A particular choice of the weighting function W can be profitable when high demanding far-field patterns are required.

the other side, the profile of the primary reflector can be determined form the residual aperture phase by exploiting inverse GO.

We consider a reflector antenna with a circular shaped aperture Σ with diameter d illuminated by a single elementary feed ($q_0 = 1$) of known excitation, say c_0 (Fig. 1). In the following, the reasoning underlying eq. (10) is still applied so that eq. (10) is assumed as the basic input-output relationship. However, taking into account that now $\underline{c}$ reduces to a known constant c_0, we assume $\mathcal{X} = \mathbf{C}^p$. It must be noted that also in this case the reference optical path could be useful f.i., to deal with intentionally defocused data.

Concerning the definition of the output space $\mathcal{Y}$, it is assumed that the observed data are the squared amplitudes of the co-polar and cross-polar components of the far field within the region Ω of the (u, v) plane. These components are supposed to be embedded in $\mathcal{L}_2(\Omega)$, so that $\mathcal{Y}$ is still given by eq. (6).

Accounting for noise and measurement errors and introducing the accuracy functions N_{co} and N_{cr}, the set $\mathcal{Y}_c$, i.e., the set of elements in $\mathcal{Y}$ compatible with the measurements is given by:

$$\mathsf{Y}_c = \left\{ (T_1, T_2) \in \mathsf{Y} \mid |T_1 - O_{co}|^2 \leq N_{co}, |T_2 - Q_{cr}|^2 \leq N_{cr} \ (u, v) \in \Omega \right\} \tag{14}$$

According to these considerations and exploiting the penalty method, the objective functional involved in the reflector diagnosis problem is expressed as:

$$F_{\alpha_1}(\underline{s}, c_0) = \|\mathsf{A}(\underline{s}, c_0) - \mathsf{P}_{\mathsf{Y}_c} \mathsf{A}(\underline{s}, c_0)\|^2_{\mathsf{L}_2(\Omega, W) \times \mathsf{L}_2(\Omega, W)} + \alpha_1 Q_1(\underline{s}) \tag{15}$$

where, as in eq. (12) the constant argument $\hat{\underline{V}}$ of A has been dropped out and α_1 is a multiplier making the contribution of $Q_1(\underline{s})$ comparable to the first term in eq. (15).

It is worth noting that, to account for struts and subreflector effects [56, 57], a suitable characteristic function P_Σ has been considered by computing the struts and subreflector spherical and plane wave shadow on the aperture field.

3. NUMERICAL ANALYSIS

To test the effectiveness of the proposed approach, both the synthesis and the diagnosis algorithms have been subjected to an extensive numerical analysis.

3.1. Synthesis of Reflector Antennas

The examples we refer herein consider a reflector antenna with $d = 20\lambda$, $z_0 = d$, a primary feeding array consisting of 5×5 Huygens elementary sources regularly spaced on a grid with a mesh size equal to $\lambda/2$. The unknown S is represented by Tchebitchev polynomials up to the 7-th degree.

Two cases concerning the synthesis of a contoured-beam are considered. In the first case, case A later on, a circular-triangular shaped beam is synthesized, while in case B a real world shaped beam covering Italy is considered.

The first problem which must be faced when constructing an Evolutionary Algorithm relies on how coding the unknowns.

The continuous nature of our problem suggested a real coding.

Concerning the reproduction operators, a roulette wheel proportional selection with elitist has been considered.

In order to get a non negative fitness function and to control the selection pressure, a "quasi-linear" scaling of the objective functional has been adopted according to the relationship eq. (21) of Part I.

An elitist has been introduced according to the considerations made in the Section 4 of Part I.

Concerning the mutation scheme, a uniform mutation on the searching space has been considered.

The last critical point to be faced when implementing an EA is the parameter settings. Obviously only heuristics rules are available to determine the population size and the parameters of reproduction operators.

As discussed in Part I, to solve the parameter set problem many Authors have proposed interesting schemes of Algorithms that, while searching the desired solution, also automatically tune the parameters or Algorithms whose parameters are the output of a meta-evolutionary algorithm. However, in our opinion these strategies are very time consuming, especially when hard optimization problems are involved, so that we preferred the manual tuning exploiting the abilities of the algorithm designer.

Obviously, the most part of the numerical analysis has been devoted to enlighten those modules of the Evolutionary Algorithm that provide better performances and to set the searching parameters, such as the mutation and the recombination probabilities. A population size as wide as possible, according to the available computing resources, has been considered.

In order to make the performance of the Evolutionary Algorithm no worse than the one of the local search approach, in the initial population we inserted an individual corresponding to the starting

point of the local search.

Let us now discuss some significant examples.

Concerning case A, the enforced design specifications require a top flat beam, within a tolerance equal to $-0.5\,\mathrm{dB}$ and $+0.5\,\mathrm{dB}$, inside the triangular-circular shaped portion of the (u, v) plane, say Ω_i, and inside an enlarged version of Ω_i, say Ω_e, respectively (see Fig. 2). Then a maximum and a minimum level equal to -30 and $-200\,\mathrm{dB}$ are prescribed outside Ω_i, and Ω_e, respectively. Since the cross-polar component should be as low as possible, only an upper bound equal to $-70\,\mathrm{dB}$ is considered.

The synthesis has been performed with both the Hybrid Evolutionary Algorithm (case A1) and the quasi-Newton optimizer (BFGS) [58] (case A2).

It is noted that the local phase of the hybrid algorithm is assigned to the same algorithm adopted in case A2.

The co-polar amplitude synthesized in case A1 is shown under Fig. 3 while the one synthesized in case A2 is presented in Fig. 4. The obtained results clearly show that the global optimizer outperforms the local one. In particular, the value of the objective functional attained in case A1 is about $10\,\mathrm{dB}$ under the one corresponding to case A2.

The cross-polar components obtained in case A1 and A2 are
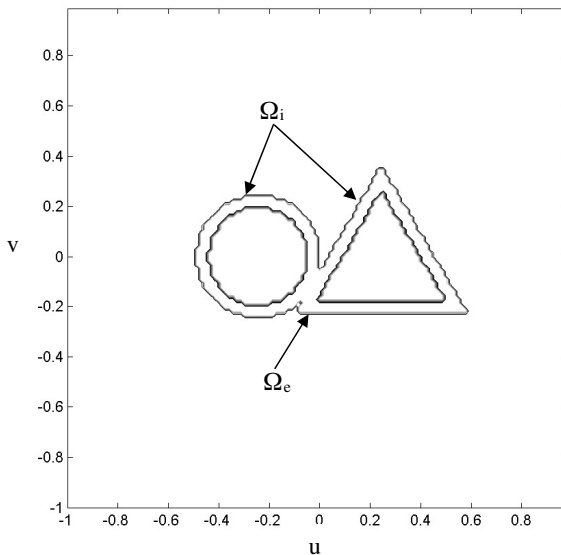
Figure 2. Boundaries of the regions Ω_i and Ω_e defining the masks in the case A.
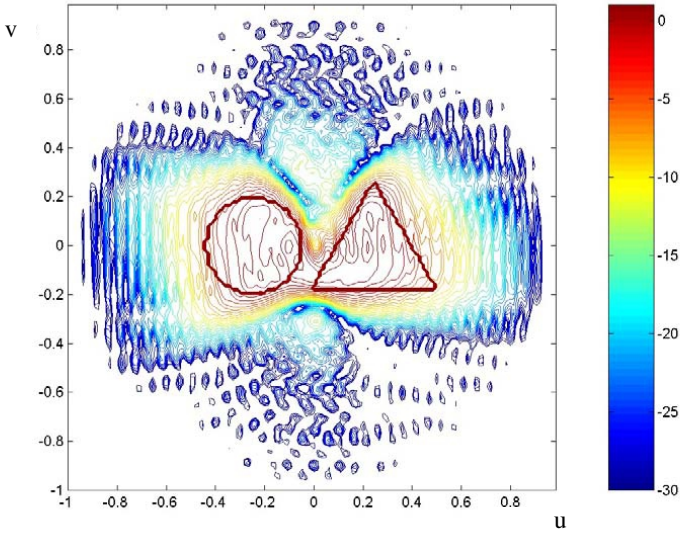
Figure 3. Co-polar synthesized by exploiting the hybrid evolutionary algorithm (case 1).
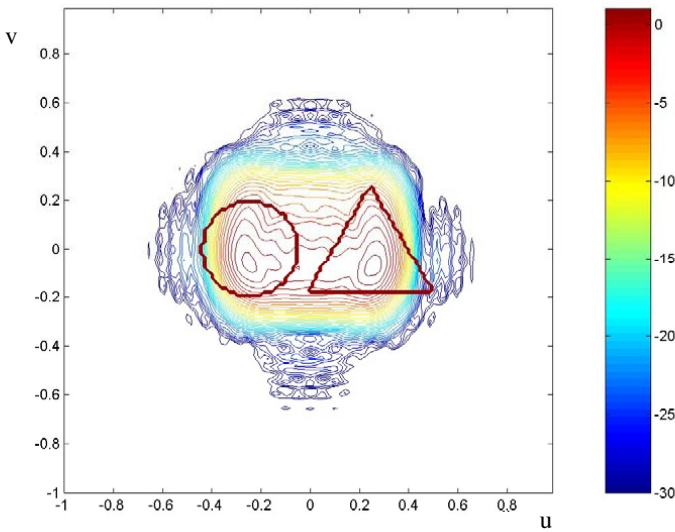

Figure 4. Co-polar synthesized by exploiting the local approach (case 1).

depicted under Figs. 5 and 6, respectively. At difference of what happens on the co-polar components, the worse result correspond now to case A1. However, the cross-polar remains under the -30 dB level.

The amplitudes and the phases of the excitations coefficients synthesized in case A1 are shown under Figs. 7 and 8, respectively, while the corresponding reflector shape is shown under Fig. 9.

As case A, case B involves a top flat beam within a tolerance equal to -0.5 and $+0.5$ dB, inside the regions of the (u, v) plane Ω_i, and Ω_e, respectively, shown in Fig. 10 and tailored to the Italian peninsula, the Sicily and Sardinia islands, also reported in that figure. Again a maximum and a minimum level equal to -30 and -200 dB are prescribed outside Ω_i and Ω_e, respectively. Since the cross-polar component should be as low as possible, only an upper bound equal to -70 dB is considered.

The synthesis has been performed with both the hybrid evolutionary algorithm (case B1) and the quasi-Newton optimizer (BFGS) (case B2).

The co-polar amplitude synthesized in case B1 is shown under Fig. 11 while the one synthesized in case B2 is presented in Fig. 12. Again, the obtained results clearly show that the global optimizer outperforms the local one. In particular, the value of the objective functional attained in case B1 is about 3 dB under the one corresponding to case B2.

The cross-polar components obtained in case B1 and in case B2 are depicted under Figs. 13 and 14, respectively. Again a worsening of the cross-polar level characterize the result obtained with the hybrid approach with respect to those corresponding to the local search. Anyway, as in case A, the result appears quite good, since the cross-polar remains under the -30 dB.

The amplitudes and the phases of the excitations coefficients synthesized in case B1 are shown under Figs. 15 and 16, respectively, while the corresponding reflector shape is shown under Fig. 17.

3.2. Diagnosis of Reflector Antennas

The main results of an extensive numerical analysis involving the reflector diagnosis algorithm are now presented.

All the worked examples have involved a parabolic reflector (in its undistorted configuration) corresponding to a real antenna of the JPL/DSN, whose diameter and working frequency are equal to 34 m and about 12 GHz, respectively.

The antenna is fed at the focus by an elementary radiator with pure co-polar y-directed primary pattern of the type $cos^m(\varphi)$ with $m = 9$, providing a tapering of about 10 dB at the reflector edge. As
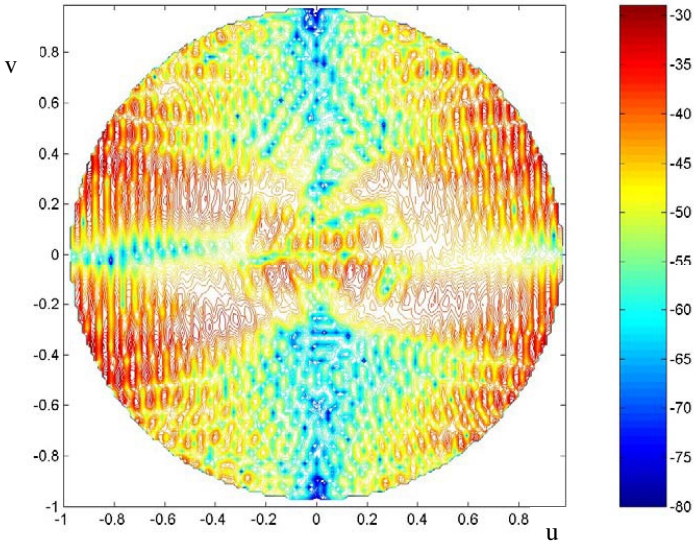
Figure 5. Cross-polar synthesized by exploiting the hybrid evolutionary algorithm (case 1).
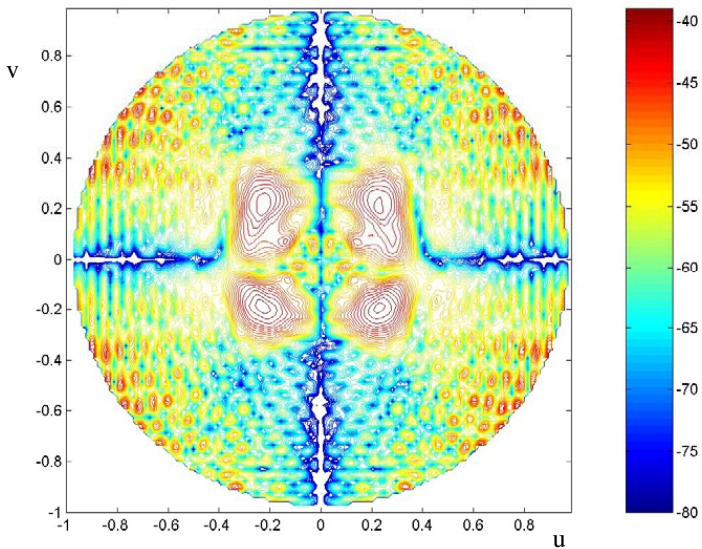

Figure 6. Cross-polar synthesized by exploiting the local approach (case 1).
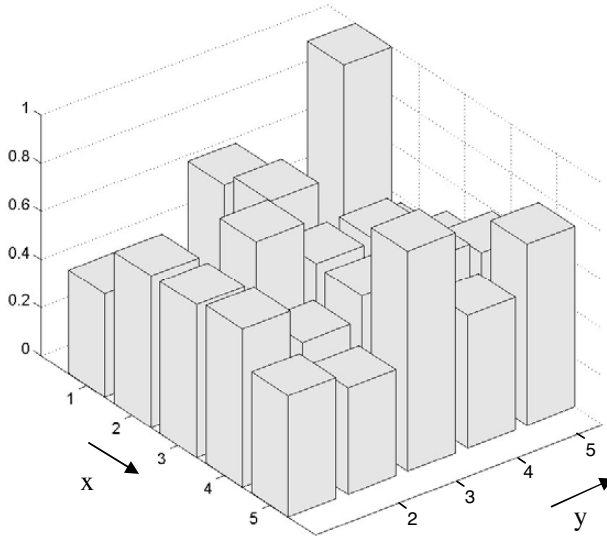
Figure 7. Amplitudes of the excitation coefficients obtained by exploiting the hybrid evolutionary algorithm (case 1).
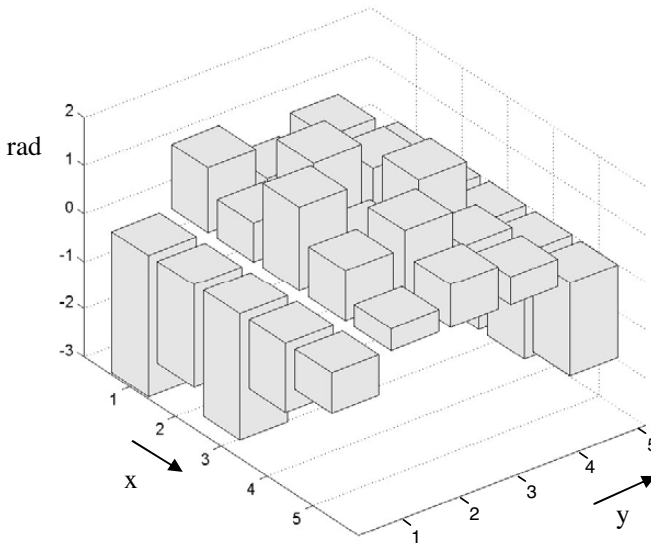

Figure 8. Phases of the excitation coefficients obtained by exploiting the hybrid evolutionary algorithm (case 1).
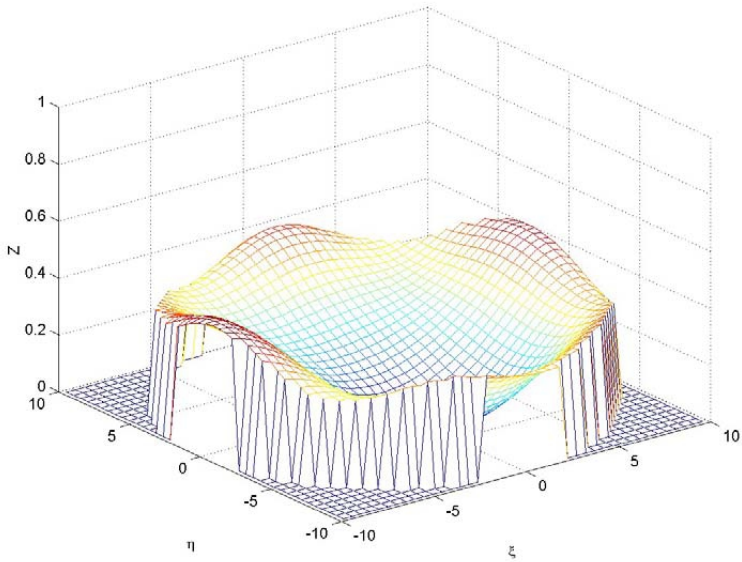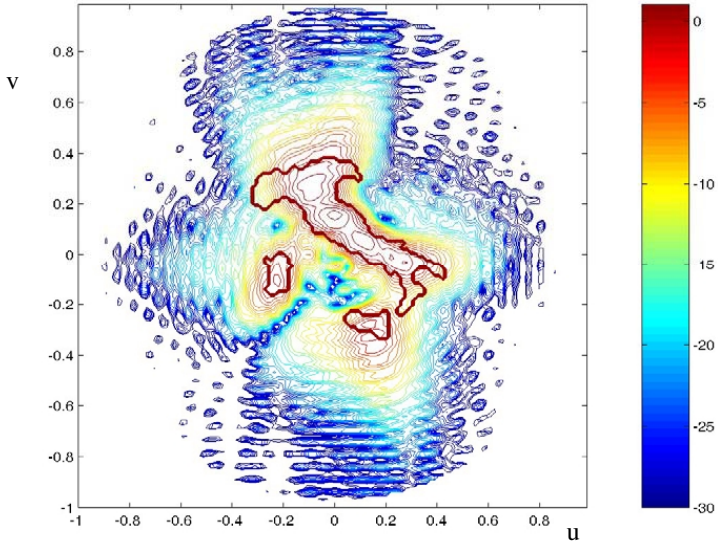
Figure 9. Reflector shape synthesized by exploiting the hybrid evolutionary algorithm (case 1).
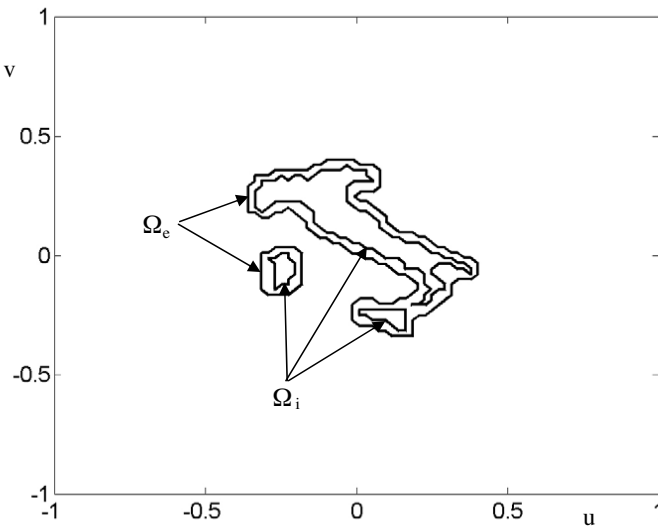
Figure 10. Boundaries of the regions Ω_j and Ω_e defining the masks in the case B.

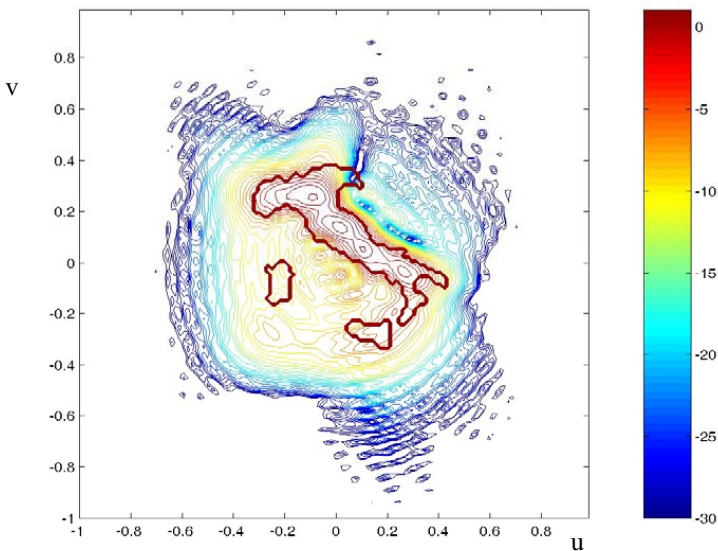**Figure 11.** Co-polar synthesized by exploiting the hybrid evolutionary algorithm (case 2).

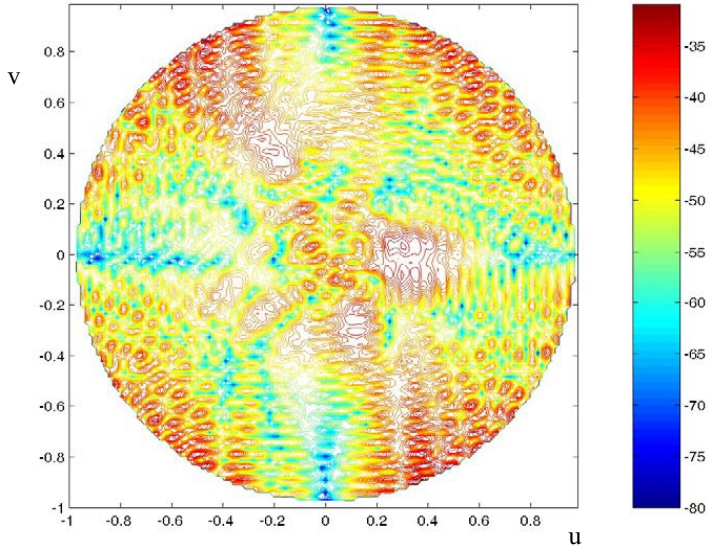**Figure 12.** Co-polar synthesized by exploiting the local approach (case 2).

Figure 13. Cross-polar synthesized by exploiting the hybrid evolutionary algorithm (case 2).
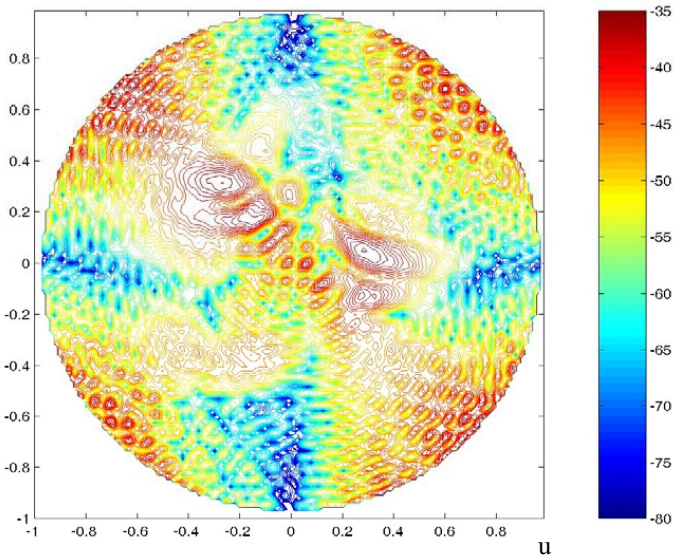

Figure 14. Cross-polar synthesized by exploiting the local approach (case 2).
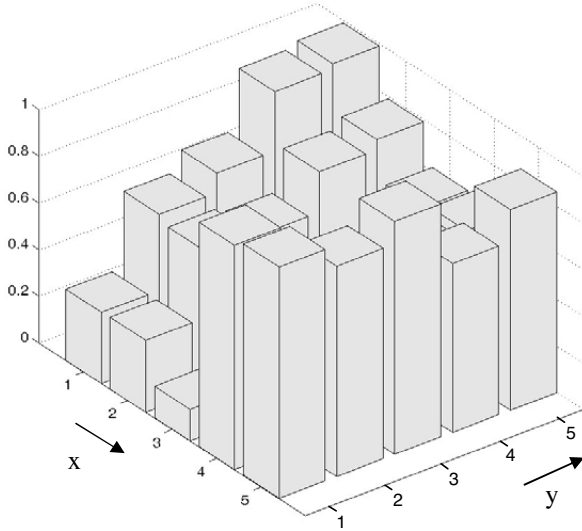
Figure 15. Amplitudes of the excitation coefficients obtained by exploiting the hybrid evolutionary algorithm (case 2).
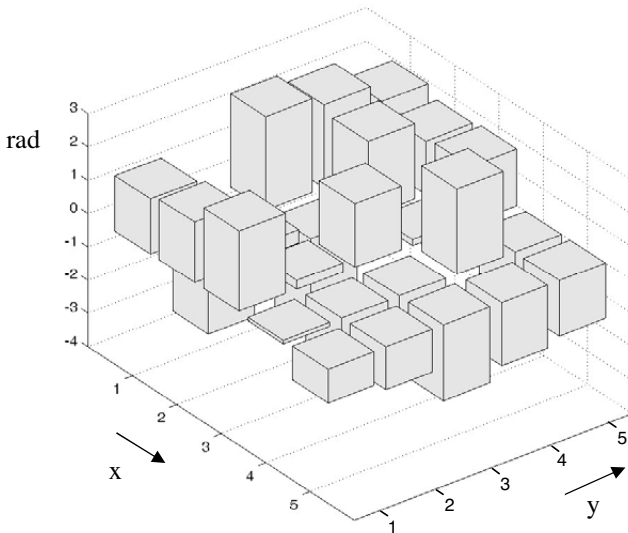

Figure 16. Phases of the excitation coefficients obtained by exploiting the hybrid evolutionary algorithm (case 2).
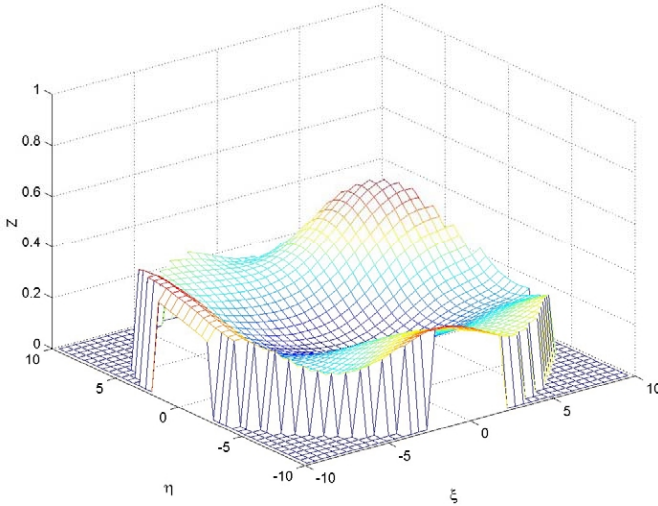
Figure 17. Reflector shape synthesized by exploiting the hybrid evolutionary algorithm (case 2).

a consequence, the x-component of $\underline{E}_a$ is zero, while the y-component is proportional to $\cos^m(\theta)(1 + cos(\theta))$.

Concerning the basis function exploited in the expansion of the optical path disturbance, we considered two different choices: the Tchebytcheff and the Zernike polynomials [59]. Obviously, both are complete in the space of square integrable functions, although the Zernike polynomials are orthogonal on the circle of unitary radius. A numerical analysis has been performed to chose the more convenient representation.

In particular, the reflector deformations have been simulated by representing the reflecting surface by means of Tchebytcheff polynomials and by randomly and uniformly generating the expansion coefficient (the simulated distortion has been suitably scaled to fix the maximum deformation).

Then, the far-field power pattern has been computed by using the current method, that differs from the aperture approach exploited in the retrieving process.

The retrieving step has been performed by using only the local algorithm and the results obtained with both representations of the optical path disturbance S have been compared. The numerical analysis showed that Zernike polynomials are more convenient than the Tchebitchev ones, since, for a fixed degree of the reflector surface

distortion, they require a smaller number of iterations and a smaller number of terms to get comparable reconstructing errors.

The second point to be faced concerns the efficient evaluation of the second term in the functional (15). This require an efficient evaluation of the derivatives of the expansion polynomials. This task has been easily accomplished by using the new recursive formulas for the first order partial derivatives of the Zernike polynomials provided in [60].

However, it must be stressed that, as long as the degree of the expansion coefficients of S is less then 9 and the range of variability of the expansion coefficient remains confined to the interval $[-1, 1]$ the eikonal constraint has never been violated in our numerical analysis.

After this preliminary study, we started the analysis of the performances of the Hybrid Algorithm.

As in the synthesis case, the most part of the numerical analysis has been devoted to enlighten those modules of the Evolutionary Algorithm that provide better performances and to set the searching parameters.

Again, to make the performance of the Evolutionary Algorithm no worse than that of the local search, we inserted the individual corresponding to the undistorted reflector in the initial population.

The performed numerical analysis involved several reflector distortions with an optical path disturbance ranging from 3λ to 4.5λ. The corresponding far-field power patterns have been simulated by exploiting the current method and the effect of the noise and measurement errors have been taken into account by superimposing an additive random error, uniformly distributed with a maximum amplitude equal to $-30\,\text{dB}$ under the peak level of the simulated co-polar amplitude.

The far-field pattern corresponding to the undistorted reflector is shown in Fig. 18.

Later on, we explicitly present only one of the handled cases, corresponding to a maximum optical path disturbance on the reflector aperture equal to 4.5λ, since the results involving the other cases are very similar.

The optical path disturbance has been represented by means of Zernike polynomials up to the 7-th degree (36 expansion coefficients).

The simulated far-field patterns and the corresponding optical path distortions are shown in Figs. 19 and 20, respectively. The differences between the simulated optical path and the one retrieved by applying the local search are displayed in Fig. 21.

Clearly, the local search was unable to retrieve the reflector distortions.
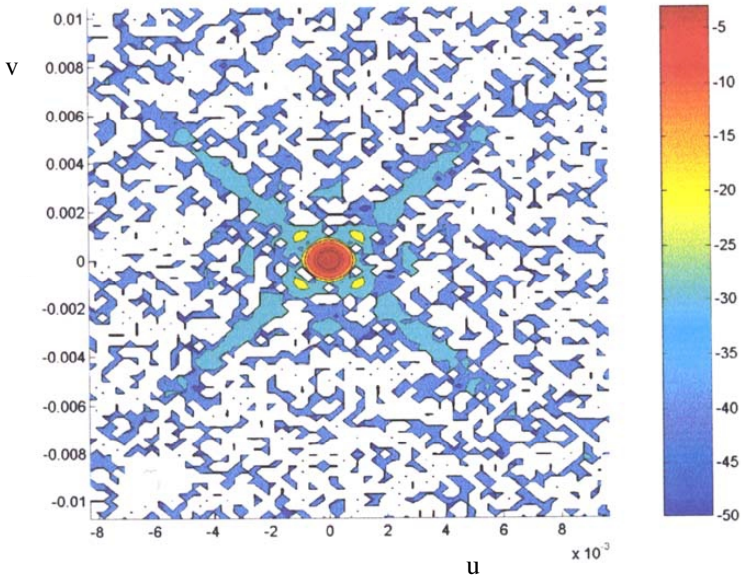
Figure 18. Squared amplitude of the copolar component radiated by the undistorted reflector.
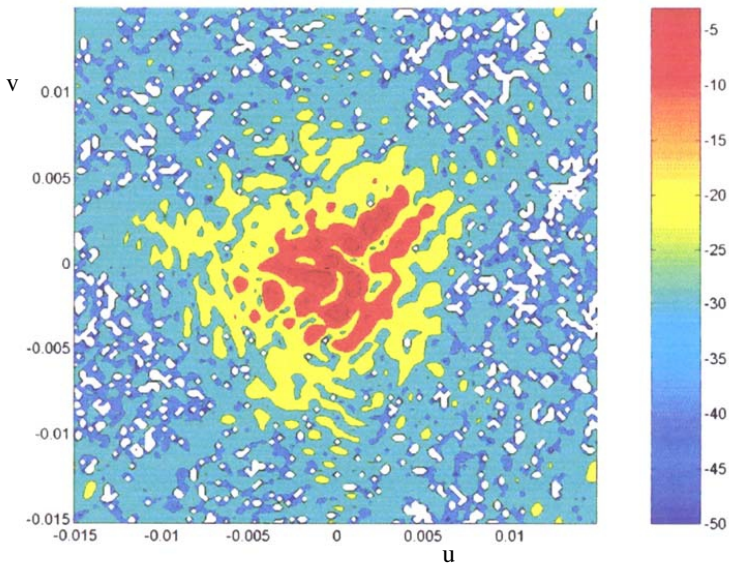

Figure 19. Squared amplitude of the copolar component radiated by the distorted reflector.
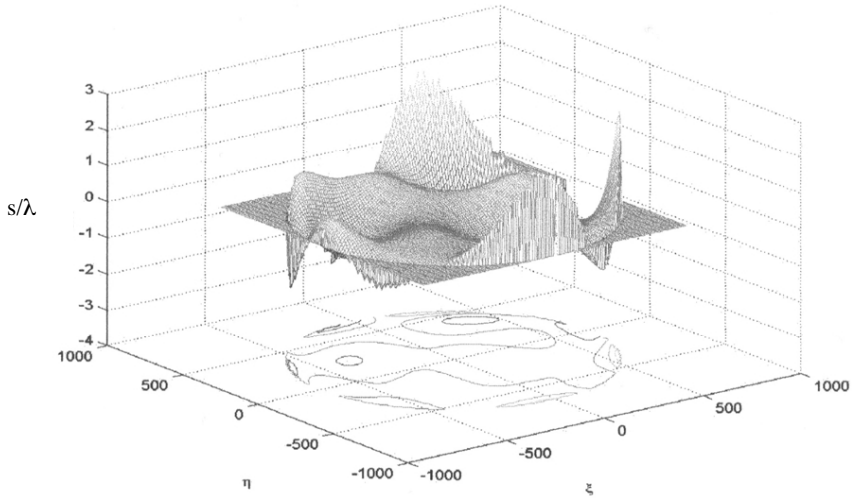
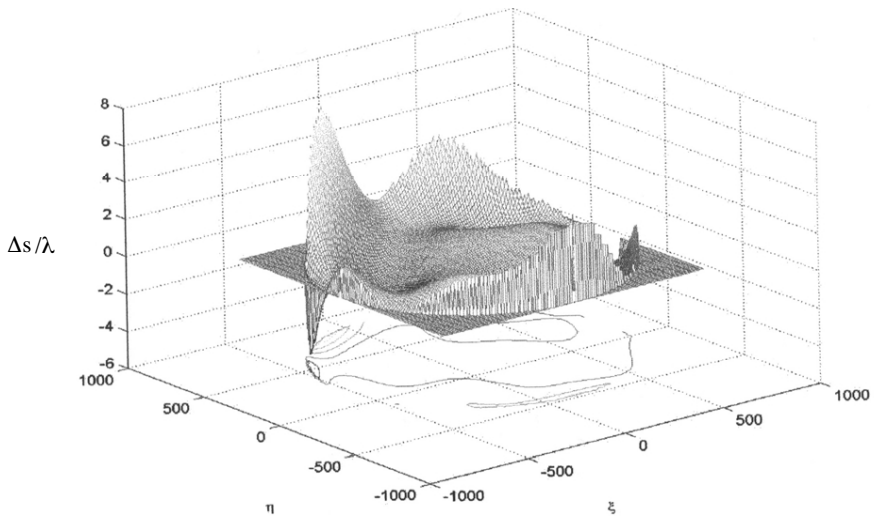**Figure 20.** Simulated optical path disturbance.

Figure 21. Difference between the simulated optical path disturbance and the one retrieved by local search algorithm.

On the other side, the difference between the path retrieved by using the Hybrid Algorithm and the true one is plotted under Fig. 22. These results show that the optical path distortions have been successfully retrieved by the Hybrid Algorithm.
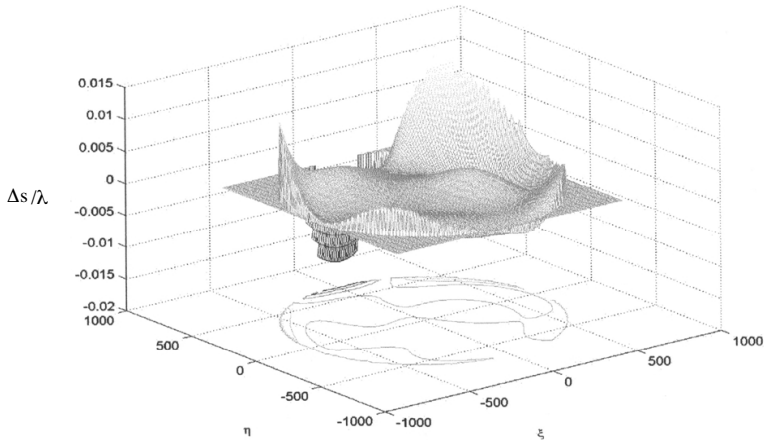

Figure 22. Difference between the simulated optical path disturbance and the one retrieved by the hybrid evolutionary algorithm.

It is worth noting that the dependence of the algorithm on the initial population has been investigated by restarting each case 5 times with different random seeds to get different initial population and a different algorithm evolution. The numerical analysis has proved that the algorithm was always able to retrieve the distortions in the 70% of the cases.

As a concluding remark, it must be stressed that, in Authors' experience, the use of the Pure Evolutionary Algorithm never allowed to attain the solution of the problem, since it requires an inordinate amount of computing time.

4. CONCLUSIONS

The application of the hybrid global optimization algorithm introduced in the Part I of the paper to two case of practical interest, the power synthesis of contoured beam hybrid reflector antennas and the reflector antenna diagnosis from only amplitude data, has been presented. To show the performances of the optimization algorithm, a numerical investigation has been performed. In both cases the global approach outperformed significantly the optimization techniques based on a local optimization tool.

REFERENCES

1. Bucci, O. M., G. D'Elia, G. Mazzarella, and G. Panariello, "Antenna pattern synthesis: a new general approach," *Proc. IEEE*, Vol. 82, No. 3, 358–371, 1994.

2. Bucci, O. M., G. D'Elia, and G. Romito, "Synthesis technique for scanning and/or reconfigurable beams reflector antennas with phase-only control," *IEE Proc. Microw. Antennas Propagat.*, Vol. 143, 402–412, 1996.

3. Shen, B. and W. L. Stutzman, "Design of sperical trireflector antennas with high aperture efficiency," *IEEE Trans. Antennas and Propagat.*, Vol. 41, No. 6, 778–786, 1993.

4. Searle, A. D. and B. S. Westcott, "Hybrid antenna synthesis for reconfigurable contoured beams," *IEE Proc. Pt. H.*, Vol. 140, No. 4, 263–268, 1993.

5. Botha, E. and D. A. McNamara, "Conformal array synthesis using alternating projections with maximal likelihood estimation used in one of the projection operator," *Electronics Letters*, Vol. 29, 1733–1734, 1993.

6. Clarricoats, P. J. B., A. D. Monk, and H. Zhou, "Array-fed reconfigurable reflectors for spacecraft systems," *Electronics Letters*, Vol. 30, No. 8, 613–614, 1994.

7. Steiskal, H., "Synthesis of antenna patterns with imposed near-field nulls," *Electronics Letters*, Vol. 30, No. 24, 2000–2001, 1994.

8. Duan, D. W. and Y. Rahmat-Samii, "A generalized diffraction synthesis technique for high performance reflector antennas," *IEEE Trans. Antennas and Propagat.*, Vol. 43, No. 1, 27–40, 1995.

9. Buckley, M. J., "Synthesis of shaped beams antenna patterns using implicitly constrained current elements," *IEEE Trans. Antennas Propagat.*, Vol. 44, 192–197, 1996.

10. Vaskelainen, L. J., "Iterative least-squares synthesis methods for conformal array antennas with optimized polarization and frequency properties," *IEEE Trans. Antennas Propagat.*, Vol. 45, No. 7, 1179–1185, 1997.

11. Landesa, L., F. Obelleiro, J. L. Rodriguez, and A. G. Pino, "Pattern synthesis of array antennas in presence of conducting bodies of arbitrary shape," *Electronics. Letters*, Vol. 33, No. 18, 1512–1513, 1997.

12. Obelleiro, F., L. Landesa, J. L. Rodriguez, A. G. Pino, and M. R. Pino, "Directivity optimisation of an array antenna with obstacles within the near-field region," *Electronics Letters*,

Vol. 33, No. 25, 2087–2088, 1997.

13. Landesa, L., F. Obelleiro, J. L. Rodriguez, J. A. Rodriguez, F. Ares, and A. G. Pino, "Pattern synthesis of array antennas with additional isolation of near-field arbitrary objects," *Electronics Letters*, Vol. 34, No. 16, 1540–1541, 1998.

14. Hay, S. G., "Dual-shaped-reflector directivity pattern synthesis using the successive projections method," *IEE Proc. Microw. Antennas Propagat.*, Vol. 146, No. 2, 119–124, 1999.

15. Hoferer, R. A. and Y. Rahmat-Samii, "A GO-subreflector implementation methodology using a Fourier-Jacobi surface expansion," *Proc. of the IEEE Antennas and Propagation Society*, Vol. 4, 2328–2331, 1999.

16. Bucci, O. M., A. Capozzoli, and G. D'Elia, "An effective power synthesis technique for shaped, double-reflector multifeed antennas," *Journal of Electromagnetic Waves and Applications* Vol. 17, No. 5, 743–754, 2003.

17. Bucci, O. M., A. Capozzoli, and G. D'Elia, "Reconfigurable conformal array synthesis with near field constraints," *PIERS 2000*, Cambridge, Massachusetts, USA, July 5–14, 2000.

18. Bucci, O. M., A. Capozzoli, and G. D'Elia, "Synthesis of reflector antennas with near-field constraints," *Proceedings of the IEEE Transactions on Antennas and Propagation Society*, Vol. 1, 562–565, 2001.

19. Bucci, O. M., A. Capozzoli, and G. D'Elia, "A global optimization technique in the synthesis of reflector antennas," *17th Annual Review of Progress in Applied Computational Electromagnetics*, March 19–23, 2001.

20. Haupt, R. L., "Thinned arrays using genetic algorithms," *IEEE Trans. Antennas and Propagat.*, Vol. 42, No. 7, 993–999, 1994.

21. Mitchell, R. J., B. Chambers, and A. P. Anderson, "Array pattern synthesis in the complex plane optimised by a genetic algorithm," *Electronics Letters*, Vol. 32, No. 20, 1843–1845, 1996.

22. Johnson, J. M. and Y. Rahmat Samii, "Genetic algorithms in engineering electromagnetics," *IEEE Antennas Propagat. Mag.*, Vol. 39, No. 4, 7–25, 1997.

23. Ferreira, J. A. and F. Ares, "Pattern synthesis of conformal arrays by the simulated annealing technique," *Electronics Letters*, Vol. 33, No. 14, 1187–1189, 1997.

24. Yan, K.-K. and Y. Lu, "Side lobe reduction in array-pattern synthesis using genetic algorithm," *IEEE Trans. Antennas and Propagat.*, Vol. 45, No. 7, 1117–1122, 1997.

25. Markus, K. and L. Vaskelainen, "Optimisation of synthesised array excitations using array polynome complex root swapping and genetic algorithms," *IEE Proc. Microw. Antennas Propagat.*, Vol. 145, No. 6, 460–464, 1998.

26. Marcano, D. and F. Duran, "Synthesis of antenna arrays using genetic algorithms," *IEEE Antennas and Propagation Magazine*, Vol. 42, No. 3, 12–20, 2000.

27. Safak, M., "Limitation on reflector antenna gain by random surface errors, pointing errors, and the angle-of arrival jitter," *IEEE Trans. Antennas and Propagat.*, Vol. 38, No. 1, 117–121, 1990.

28. Rochblatt, D. J. and Y. Rahamat-Samii, "Effects of measurement Errors on microwave antenna holography," *IEEE Trans. Antennas and Propagat.*, Vol. 39, No. 7, 933–942, 1991.

29. Ramson, P. L. and R. Mittra, "A method for locating defective elements in large phased array," *Phased Arrays*, A. A. Oliner and G. H. Knitt (Eds.), 351–356, 1972.

30. Bennet, J. C, A. P. Anderson, P. A. McInnes, and A. J. T. Whitaker, "Microwave holographic metrology of large reflector antennas," *IEEE Trans. Antennas and Propagat.*, Vol. 24, No. 5, 293–303, 1976.

31. Rahamat-Samii, Y., "Surface diagnosis of large reflector antennas using microwave holographic metrology: an iterative approach," *Radio Science*, Vol. 19, No. 5, 1205–1217, 1984.

32. Rahamat-Samii, Y., "Microwave holography of large reflector antennas-simulation algorithms," *IEEE Trans. Antennas and Propagat.*, Vol. 33, No. 11, 1194–1203, 1985.

33. Morris, D., "Phase retrieval in the radio holography of reflector antennas and radio telescopes," *IEEE Trans. Antennas and Propagat.*, Vol. 33, No. 7, 749–755, 1985.

34. Morris, D., "Correction to: phase retrieval in the radio holography of reflector antennas and radio telescopes," *IEEE Trans. Antennas and Propagat.*, Vol. 33, No. 12, 1419, 1985.

35. Anderson, A. P. and S. Sali, "New possibilities for phaseless microwave diagnostics. Part 1: Error reduction techniques," *IEE Proceedings Pt. H*, Vol. 132, No. 5, 291–298, 1985.

36. Gardenier, P. H., C. A. Lim, D. G. H. Tan, and R. H. T. Bates, "Aperture distribution phase from single radiation pattern measurement via Gerchberg-Saxton algorithm," *Electronic Letters*, Vol. 22, No. 2, 113–115, 1986.

37. Rahamat-Sarnii, Y., "Correction to: microwave holography of

260 Capozzoli and D'Elia

large reflector antennas-simulation algorithms," *IEEE Trans. Antennas and Propagat.*, Vol. 34, No. 6, 853, 1986.

38. Morris, D., H. Hein, H. Steppe, and J. W. M. Baars, "Phase retrieval radio holography in the Fresnel region: tests on the 30 m telescope at 86 GHz," *IEE Proceedings Pt. H*, Vol. 135, No. 1, 61–64, 1988.

39. Anderson, A. P. and J. E. M. McCorrnack, "Phase retrieval enhancement of antenna metrology data," *Electronic Letters*, Vol. 24, No. 19, 1243–1244, 1988.

40. Rochblatt, D. J. and Y. Rahamat-Samii, "Effects of measurement errors on microwave antenna holography," *IEEE Trans. Antennas and Propagat.*, Vol. 39, No. 7, 933–942, 1991.

41. Wood, P. J., "A new methodology for reconstructing aperture field from spherical surface data, with application to the array diagnostic," *IEEE Trans. Antennas and Propagat.*, Vol. 39, 1436–1441, 1991.

42. Morris, D., J. H. Davis, and C. E. Mayer, "Experimental assessment of phase retrieval holography of radiotelescope," *IEE Proceedings Pt. H*, Vol. 138, No. 3, 243–247, 1991.

43. Morris, D., "Simulated annealing applied to the Misell algorithm for phase retrieval," *IEE Proceedings Pt. H*, Vol. 143, No. 4, 298–303, 1991.

44. Anderson, A. P., Y. D. Cheung, and J. Junkin, "Phase retrieval near-field metrology of unknown aperture," *Electronic Letters*, Vol. 28, No. 5, 454–455, 1992.

45. Lord, J. A., G. G. Cook, and A. P. Anderson, "Reconstruction of the excitation of an array antenna from measured near-field intensity using phase retrieval," *IEE Proceedings-Pt. H*, Vol. 139, No. 4, 392–396, 1992.

46. Rochblatt, D. J., P. M. Withington, and H. J. Jackson, "DSS-24 microwave holography measurement," NASA/JPL TDA Progress Report, 1995.

47. Richter, P. H. and D. J. Rochblatt, "A microwave performance calibration system for NASA's deep space network antennas, Part 1: Assessment of antenna gain and pointing, and calibration of radio sources," *10th International Conference on Antennas and Propagation*, Edinburgh, April 1997.

48. Rochblatt, D. J., P. H. Richter, and T. Y. Otoshi, "A microwave performance calibration system for NASA's deep space network antennas, Part 2: Holography, alignment, and frequency stability," *10th International Conference on Antennas*

and Propagation, Edinburgh, April 1997.

49. Leone, G. and R. Pierri, "Reflector antenna diagnosis from phaseless data," *IEEE Trans. Antennas and Propagat.*, Vol. 45, No. 8, 1236–1244, 1997.

50. Bucci, O. M., G. D'Elia, and G. Romito, "Reflector distortions diagnosis from far-field amplitude pattern," *IEEE Trans. Antennas and Propagat.*, Vol. 43, No. 11, 1217–1225, 1995.

51. Bucci, O. M., A. Capozzoli, and G. D'Elia, "A hybrid evolutionary algorithm in the diagnosis of reflector distortions," *JINA 98, International Symposium on Antennas*, Nizza, Francia, November 17–19, 1998.

52. Bucci, O. M., A. Capozzoli, and G. D'Elia, "A hybrid evolutionary algorithm in the diagnosis of reflector distortions from far-field amplitude pattern," *Atti della Fondazione Ronchi*, Vol. 54, No. 3, 503–519, 1999.

53. Bucci, O. M., A. Capozzoli, and G. D'Elia, "A Lamarckian — type evolutionary algorithm for large reflector diagnosis," *XXVI General Assembly of the International Union of Radio Science*, Toronto, Canada, August 13–21, 1999.

54. Bucci, O. M., A. Capozzoli, and G. D'Elia, "Diagnosis of array faults from far-field amplitude-only data," *IEEE Trans. Antennas and Propagat.*, Vol. 48, 5, 647–652, 2000.

55. Tikhonov, A. and V. Arsenine, *Methodes de Resolution de Problemes Mal Poses*, MIR, 1976.

56. Lamb, J. W. and A. D. Olver, "Blockage due to subreflector supports in large radiotelescopes antennas," *IEE Proceedings*, 133, Pt. H, 1, 43–49, 1986.

57. Moldsvor, A. and P. Kildal, "Analysis of aperture blockage in reflector antennas by using obstacle-located blockage currents," *IEEE Transactions on Antennas and Propagation*, Vol. 40, 1, 1992.

58. Luenberger, D. G., *Linear and Nonlinear Programming*, Addison-Wesley, 1984.

59. Born, M. and M. Wolf, *Principles of Optics*, Pergamon Press, 1970.

60. Capozzoli, A., "On a new recursive formula for zernike polynomials first order derivatives," *Atti della Fondazione G. Ronchi, Anno LIV*, No. 6, Novembre–Dicembre 1999.